ORIGINAL ARTICLE

Methyltransferase SETD2 inhibits tumor growth and metastasis via STAT1–IL-8 signaling-mediated epithelial–mesenchymal transition in lung adenocarcinoma

Xin Yang[1,2,3] | Rui Chen[1] | Yan Chen[1] | You Zhou[2,3,4] | Chen Wu[1] | Qing Li[5] | Jun Wu[1] | Wen-wei Hu[1] | Wei-qing Zhao[1] | Wei Wei[1] | Jun-tao Shi[6] | Mei Ji[1]

[1]Department of Oncology, The Third Affiliated Hospital of Soochow University, Changzhou, China

[2]Jiangsu Engineering Research Center for Tumor Immunotherapy, Changzhou, China

[3]Institute of Cell Therapy, Soochow University, Changzhou, China

[4]Department of Tumor Biological Treatment, The Third Affiliated Hospital of Soochow University, Changzhou, China

[5]Department of Pathology, The Third Affiliated Hospital of Soochow University, Changzhou, China

[6]Department of Cardiothoracic Surgery, The Third Affiliated Hospital of Soochow University, Changzhou, China

Correspondence
Jun-tao Shi, Department of Cardiothoracic Surgery, the Third Affiliated Hospital of Soochow University, No. 185 Juqian Road, Tianning District, Changzhou 213000, China.
Email: cmusjt@126.com

Mei Ji, Xin Yang, Department of Oncology, the Third Affiliated Hospital of Soochow University, No. 185 Juqian Road, Tianning District, Changzhou 213000, China.
Emails: zlkjimei@163.com; yangxindoctor@163.com

Abstract

Lung adenocarcinoma (LUAD) is a major subtype of non–small-cell lung cancer, which is the leading cause of cancer death worldwide. The histone H3K36 methyltransferase SETD2 has been reported to be frequently mutated or deleted in types of human cancer. However, the functions of SETD2 in tumor growth and metastasis in LUAD has not been well illustrated. Here, we found that SETD2 was significantly downregulated in human lung cancer and greatly impaired proliferation, migration, and invasion *in vitro* and *in vivo*. Furthermore, we found that SETD2 overexpression significantly attenuated the epithelial–mesenchymal transition (EMT) of LUAD cells. RNA-seq analysis identified differentially expressed transcripts that showed an elevated level of interleukin 8 (IL-8) in STED2-knockdown LUAD cells, which was further verified using qPCR, western blot, and promoter luciferase report assay. Mechanically, SETD2-mediated H3K36me3 prevented assembly of Stat1 on the *IL-8* promoter and contributed to the inhibition of tumorigenesis in LUAD. Our findings highlight the suppressive role of SETD2/H3K36me3 in cell proliferation, migration, invasion, and EMT during LUAD carcinogenesis, via regulation of the STAT1–IL-8 signaling pathway. Therefore, our studies on the molecular mechanism of SETD2 will advance our understanding of epigenetic dysregulation at LUAD progression.

KEYWORDS
EMT, IL-8, lung adenocarcinoma, SETD2, Stat1

----

1 | INTRODUCTION

Lung cancer remains one of the deadliest malignancies worldwide.[1-3] Most patients have advanced NSCLC. Histologically, it can be divided into lung adenocarcinoma (LUAD) and squamous cell carcinoma, between which LUAD is the most common subtype, accounting for more than 70% of NSCLC.[4] Despite tremendous advances in chemotherapy and radiation over the past few decades, the outlook for LUAD patients is bleak, with just over 15% surviving for 5 years after diagnosis.[5,6] Therefore, there is an urgent need to unveil underlying mechanisms and develop new therapeutic strategies to improve the treatment of LUAD.

Epigenetics is defined as heritable changes in gene expression, not as a result of changes in DNA sequence.[7] Over the past few years, it has become increasingly clear that dysfunctional epigenetic regulatory processes play a central role in the development and progression of cancer.[8,9] In contrast with DNA mutations, epigenetic modifications are reversible and therefore suitable for drug intervention.[10] Reversible histone methylation is an important process in epigenetic regulation and its role in cancer has made lysine methyltransferase and demethylase promising targets for new anticancer drugs.[11] Set domain-containing 2 (SETD2) is a major mammalian methyltransferase, responsible for catalyzing the trimethylation of histone 3 on lysine 36 (H3K36me3).[12,13] The SETD2 mutation has been found in colorectal cancer, renal clear cell carcinoma, breast cancer, glioma, acute leukemia, chronic lymphocytic leukemia, and other tumors.[13-15] Previous studies have identified that SETD2 and its dependent H3K36me3 both participate in both active or suppressed transcriptional regulation in a series of cellular processes reviewed previously.[16] SETD2-mediated H3K36me3 can prevent the initiation of spurious transcription by recruiting histone deacetylase complexes, and depletion of Set2 results in increased levels of this adverse transcription.[17,18] In recent decades, research on SETD2 dysfunction has been ongoing in order to explore its role in NSCLC progression.[15,19-21] However, the underlying mechanism of SETD2 in the pathological progression of LUAD is largely unknown.

Here, combined with data mining of public patient data sets and human LUAD tissue arrays, we mainly utilized lung cancer cell lines to establish that SETD2 functions as a putative tumor suppressor in LUAD. Mechanistic investigation indicated that SETD2 and its mediated H3K36me3 negatively regulate IL-8 transcription in a Stat1-dependent manner. Consequently, SETD2 ablation upregulates IL-8 expression to stimulate EMT progression to promote tumorigenesis in LUAD. Therefore, our results highlight that patients with SETD2 loss exhibit worse clinical outcomes with potentially therapeutic implications in LUAD.

2 | MATERIALS AND METHODS

2.1 | Expression plasmids and siRNA

Full-length human SETD2 and IL-8 cDNA were cloned into the pLVX-IRES-Puro vector (Clontech) to generate SETD2 and IL-8 expression plasmids, respectively. The siRNA targeting SETD2 was purchased from GenePharma. The siRNA sequences are listed as follows: siSETD2-1: 5′-CCGGAGTAGTGCTTCCCGTTATAAA-3′; siSETD2-2: 5′-CCGGACGAATTAAAGACCGCAATAA-3′; siSETD2-3: 5′-CCGGT TCCGACGAGGGTCATCATAT-3′.

2.2 | Cell line culture and reagents

All cells in this study were obtained from the Chinese Cell Bank of the Chinese Academy of Sciences (Shanghai, China). Human bronchial epithelial cells HBE and human lung cancer cells A549 and H1975 were cultured in RPMI 1640 culture medium supplemented with 10% fetal bovine serum and 1% penicillin/streptomycin (P/S) solution. Lentivirus was used to establish individual stable cell lines. siRNA duplexes targeting SETD2 (100 nM) and corresponding negative control (NC) oligonucleotides were transfected into cells mediated by Lipofectamine 3000 (Invitrogen) according to the manufacturer's instructions.
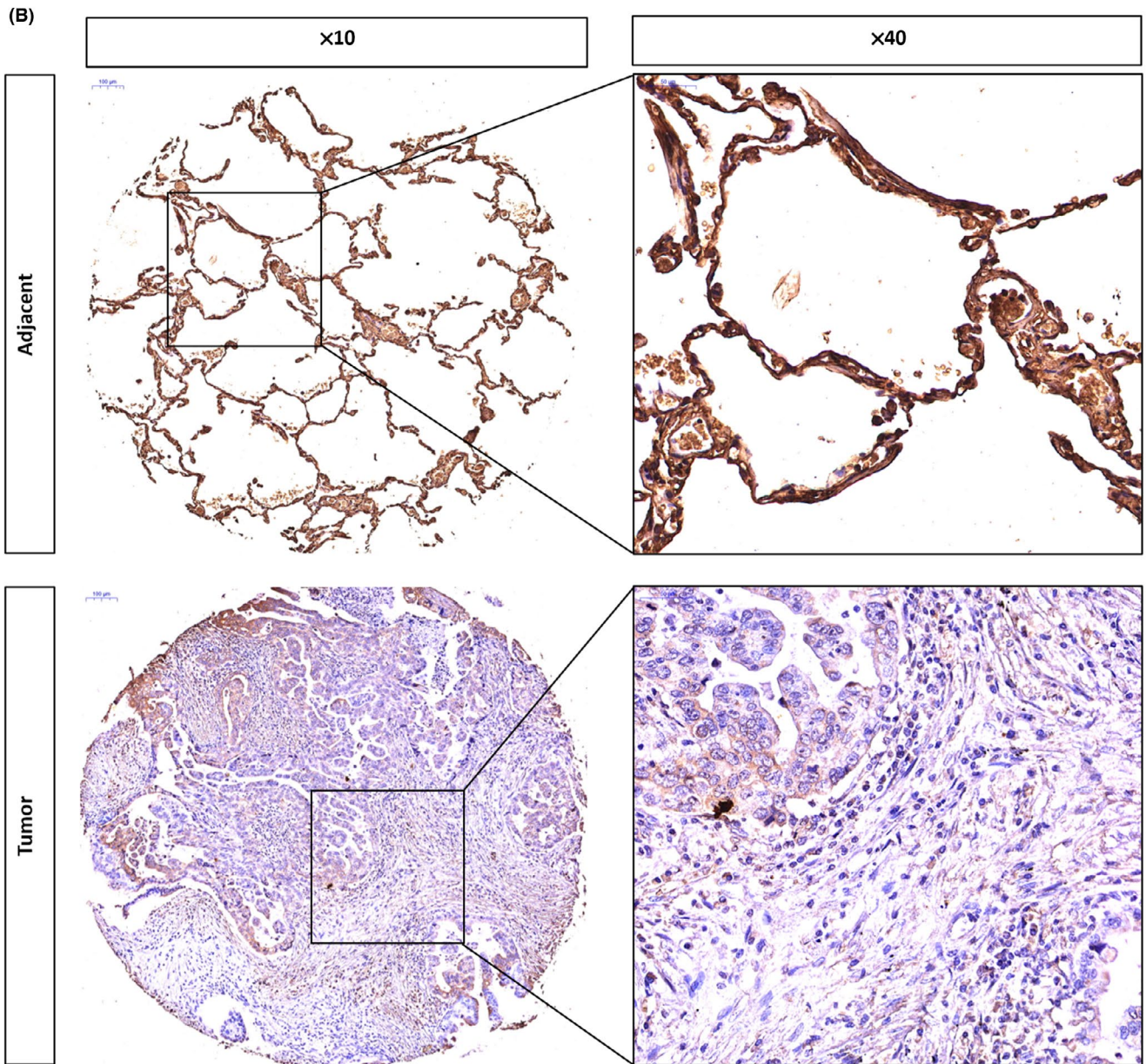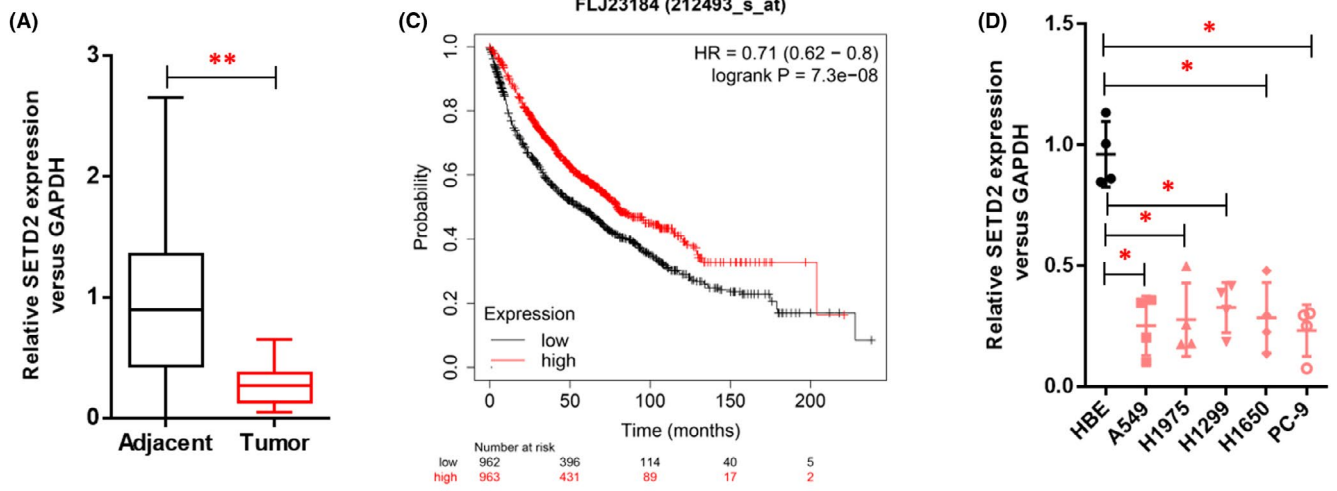
2.3 | RNA isolation and real-time qPCR

Total RNA was extracted using TRIzol reagent according to the manufacturer's instructions. First-strand cDNA was synthesized using Superscript II (Invitrogen) and 1 μg of total RNA was used in each cDNA synthesis reaction. SYBR green Universal Master Mix reagent (Roche) and primer mixtures were used for real-time qPCR. GAPDH was used as the internal reference for mRNAs.

2.4 | Western blotting analyses

Total proteins were extracted and separated using SDS-PAGE gels. Anti-SETD2 antibody (Invitrogen), anti-E-cadherin antibody (Cell Signaling Technology), anti-vimentin antibody (Abcam), and H3K36me3 antibody (Cell Signaling Technology) were used at a concentration of 1:2000. H3 antibody (Cell Signaling Technology, 1:2000) and GAPDH antibody (Santa Cruz Biotechnology, 1:2000) were used as loading controls.

FIGURE 1 SETD2 expression is downregulated in human lung cancer. (A) The mRNA expression differences for SETD2 between LUAD tissues and matched tumor-adjacent tissues were analyzed using real-time PCR. (B) Protein levels of SETD2 in LUAD tissues and matched tumor-adjacent tissues were analyzed using IHC. (C) Kaplan–Meier analyses were conducted to explore the correlation of SETD2 expression with overall survival of NSCLC patients. (D) mRNA expression differences for SETD2 between human lung cancer cell lines (A549, H1975, H1299, H1650, and PC-9) and human bronchial epithelial cell line HBE. Data are presented as means ± SEM; statistical significance: *$p < 0.05$; **$p < 0.01$

(A)

(C)

FLJ23184 (212493_s_at)

HR = 0.71 (0.62 − 0.8)
logrank P = 7.3e−08

Expression
— low
— high

	Number at risk				
low	962	396	114	40	5
high	963	431	89	17	2

(D)

(B)

×10

×40

Adjacent

Tumor

2.5 | Cell proliferation assay

Cell proliferation assay was performed using CellTiter 96® Non-Radioactive Cell Proliferation Assay (CCK-8) kit (Dojindo) according to the manufacturer's instructions. Cells (1×10^4 cells/ml) were seeded into a 96-well plate (100 μl/well) and cultured in an incubator with 5% CO_2 at 37°C. Each well was supplemented with 10 μl CCK-8 solution and then incubated at 37°C for 2 h. The spectrophotometric absorbance at 590 nm was measured for each sample. All experiments were repeated three times in triplicate.

For soft agar colony formation assays, cells were suspended in RPMI 1640 medium containing 0.35% low-melting agar (Invitrogen) and 10% FBS and seeded onto a coating of 0.8% low-melting agar in RPMI 1640 medium containing 10% FBS. Plates were incubated at 37°C and 5% CO_2. Colonies were counted after a 3-week or 4-week culture. Triplicates were required for each experiment.

2.6 | Wound healing assay

The evaluation of cell migration ability was performed using a wound scrape assay to examine the role of SETD2 and IL-8 in the regulation of the migration ability of LUAD cell lines as described previously.[20]

2.7 | Transwell invasion assay

The transwell culture system was performed to examine the invasive ability of SETD2 and IL-8 on LUAD cell lines as described previously.[20]

2.8 | Reporter vector construction and luciferase reporter assays

Five *IL-8* promoter truncations containing the respective −3.0 k, −2.5 k, −2.0 k, −1.5 k and −1.0 k regions of the *IL-8* promoter were amplified and cloned into pGL3-basic vectors (Promega) to construct specific *IL-8* promoter luciferase reporter vectors.

siNC or siSETD2 was co-transfected with distinct *IL-8* promoter reporter vectors into A549 and H1975 cells using Lipofectamine 3000 (Invitrogen). The luciferase activity was measured at 48 h after transfection using the Dual Luciferase Reporter Assay System (Promega) according to the manufacturer's instructions. Triplicates were required for each experiment.

2.9 | RNA-seq and data analysis

HiSeq RNA-seq was used to detect total RNA with or without the SETD2 deletion in A549 cells. Transcriptome reads from the RNA-seq assay were mapped to the reference genome (HG19) using the *bow tie* tool. The gene expression level was quantified using the *RSEM* software package. Significance was treated by setting the *p*-value threshold to 0.05. Differentially expressed genes were then analyzed using the *clusterProfile* software package to enrich for biological pathways.
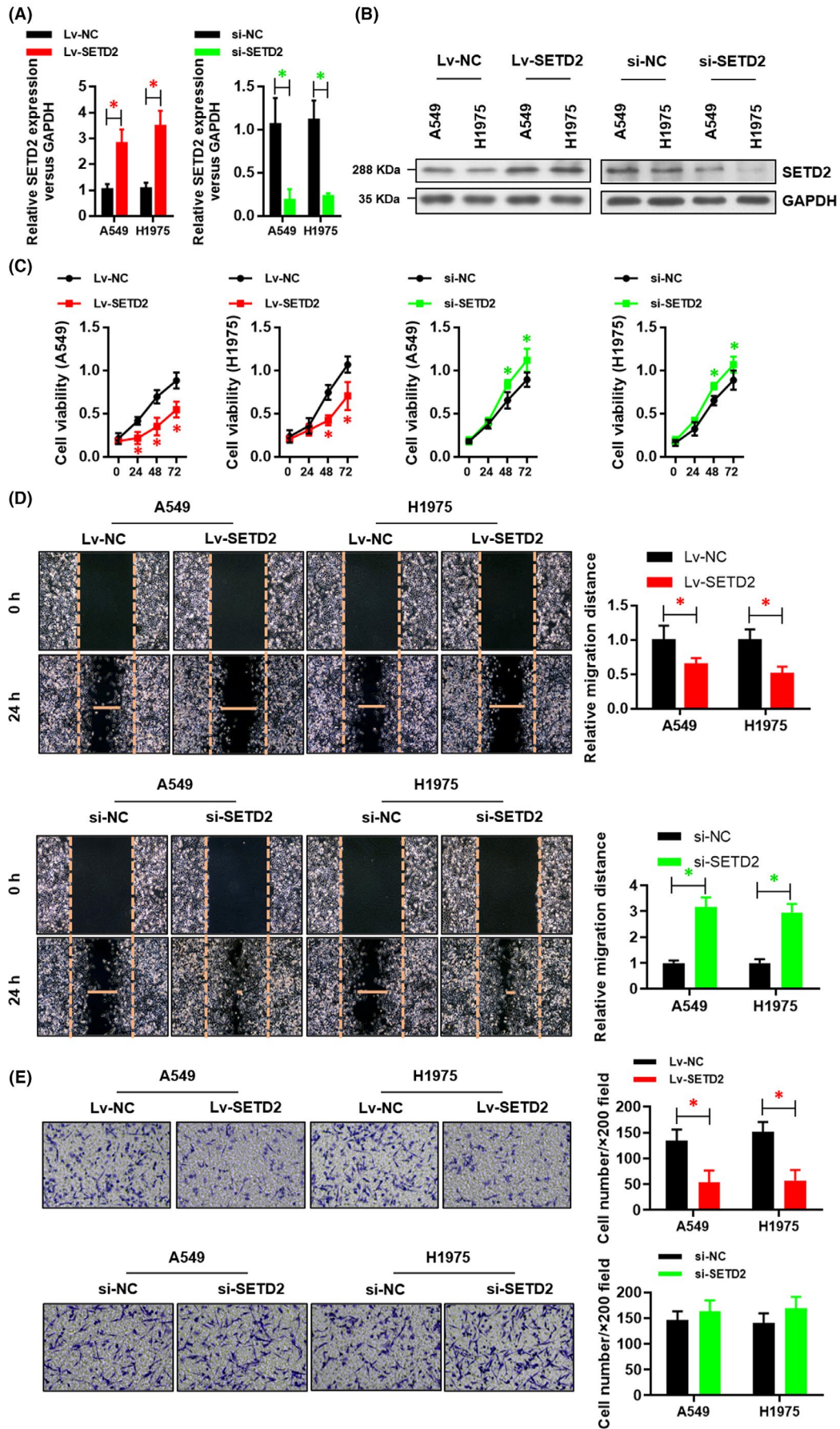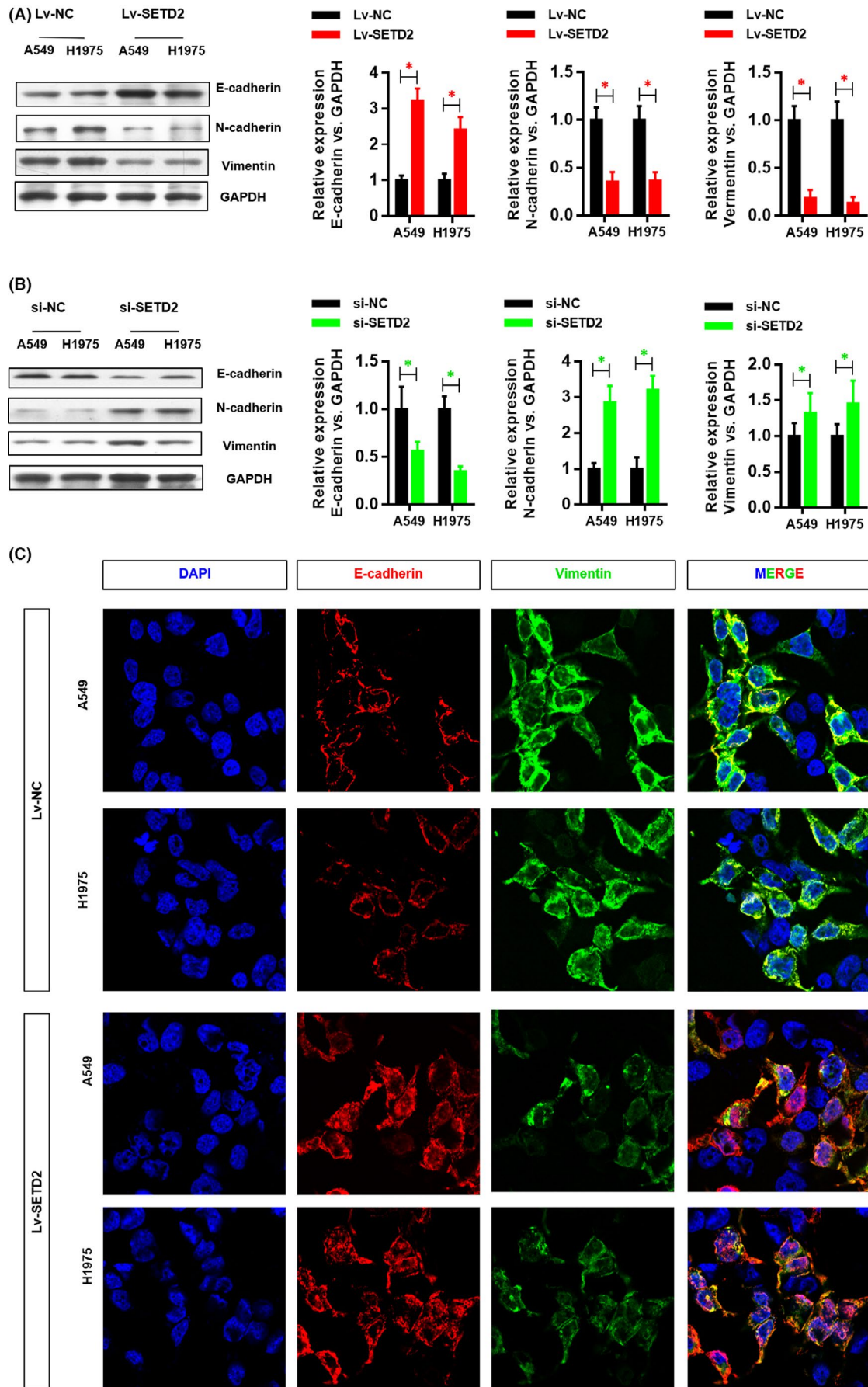
2.10 | Co-immunoprecipitation

Co-immunoprecipitation experiments were conducted using the methods described previously. Anti-SETD2, anti-H3K36me2, and anti-p-STAT1 antibodies (10 μg) were used individually for the co-immunoprecipitation experiments with normal or SETD2-knockdown A549/H1975 cells lysates. The mixture of antibodies and powders dissolved products was incubated at room temperature during a 50-min rotation and immunoprecipitation reaction of antibodies was performed by adding 50 μl protein A–Sepharose (Sigma-Aldrich) from 50% (W/V) and phosphate mud at room temperature for 30 min. The protein A–Sepharose–antibody protein complex was centrifuged at 2000 *g* for 5 min at 4°C in a chilled microcentrifuge, and the supernatant was discarded. Beads were washed with PBS five times. The washed beads were boiled in SDS loading buffer, separated by SDS-PAGE, and then analyzed using western blotting.

2.11 | ChIP assays

ChIP assays were performed using the Magnetic ChIP kit (Millipore) according to the manufacturer's instructions. Briefly, A549 and H1975 cells were fixed in 1% formaldehyde, then fragmented by a combination of MNase and sonication. ChIP grade anti-SETD2, anti-Stat1, and anti-H3K36me3 antibodies were then used for immunoprecipitation. After washing and reverse crosslinking, the precipitated DNA was amplified using *IL-8* promoter primers and then

FIGURE 2 SETD2 inhibits the cell proliferation, migration, and invasion abilities of LUAD cells *in vitro*. (A) The efficiency of overexpression and knockdown of SETD2 was confirmed using real-time PCR. (B) The efficiency of overexpression and knockdown of SETD2 was confirmed using western blot. (C) The effect of SETD2 overexpression and knockdown on the cell proliferation ability of A549 and H1975 cells was analyzed using CCK-8 assay. (D) The effect of SETD2 overexpression and knockdown on the cell migration ability of A549 and H1975 cells was analyzed using wound healing assay. (E) The effect of SETD2 overexpression and knockdown on the cell invasion ability of A549 and H1975 cells was analyzed using transwell invasion assay. Data are presented as means ± SEM, $n = 3$; statistical significance: *$p < 0.05$, **$p < 0.01$

(A)

(B)

(C)

(D)

(E)

(A)

(B)

(C)

| | DAPI | E-cadherin | Vimentin | MERGE |

quantified using a Step One Plus real-time PCR machine and DNA gel electrophoresis, respectively.

2.12 | Immunohistochemistry assays

Tumors from xenograft models were collected and then embedded in paraffin after being fixed in 4% paraformaldehyde (PFA). Immunohistochemistry (IHC) analyses were performed using specific anti-SETD2 (Invitrogen) and anti-vimentin (Abcam) antibodies.

2.13 | Xenograft tumor model

Here, 5-week-old BALB/c nude mice was purchased from the SLAC Animal Center (Shanghai, China) and then used for the xenograft tumor model. A549 cells were injected subcutaneously into nude mice and then tumor volumes were monitored every 5 days. Tumor volumes were estimated by length and width and calculated using the following formula:

$$\text{Tumor volume} = \left(\text{length} * \text{width}^2\right)/2$$

At ~1 month later, the nude mice were sacrificed and then tumors were excised, photographed, and weighed.

2.14 | Statistical analysis

All experiments were performed using three independent repeated experiments with cells. GraphPad Prism 8.0 software was applied for statistical analyses. Data in all figures are presented as the mean ± SEM. Statistical significance was determined using multiple t-test, one-way ANOVA, two-way ANOVA, Pearson correlation coefficients, or log-rank test. For all statistical tests, the 0.05 level of confidence (two-sided) was accepted for statistical significance.

3 | RESULTS

3.1 | SETD2 expression is downregulated in human lung cancer

To explore the possible role of SETD2 in lung cancer, data mining using a public data set indicated that SETD2 expression was decreased in tumors compared with the normal counterparts

(Figure 1A). Moreover, the SETD2 expression pattern was also examined using human LUAD tissue array. Results showed that the expression level of SETD2 was significantly decreased in tumors compared with normal adjacent lung epithelial tissues (Figure 1B). The survival analysis using KM Plot (http://kmplot.com/) also demonstrated that the patients with low expression of SETD2 had a poor prognosis (Figure 1C). Similarly, human lung cancer cell lines (A549, H1975, H1299, H1650 and PC-9) showed a significantly lower expression of SETD2 compared with human bronchial epithelial cell line HBE (Figure 1D). Together, these findings highlighted SETD2 as a prognostic biomarker for LUAD patients and the causal role of SETD2 in tumorigenesis of lung cancer.

3.2 | SETD2 impairs proliferation, migration, and invasion ability of LUAD cells

To investigate the biological roles of SETD2 in LUAD, we first ectopically overexpressed and silenced SETD2 in lung cancer cells A549 and H1975. Real-time qPCR (Figure 2A) and western blotting (Figure 2B) analyses were performed to confirm the overexpression of SETD2. We found that increased expression of SETD2 significantly attenuated cell proliferation (Figure 2C), migration (Figure 2D), and invasion (Figure 2E) in A549 and H1975 LUAD cells, whereas silencing of SETD2 improved these features (except invasion). Together, our results indicated that SETD2 impaired proliferation, migration, and invasion ability of LUAD cells.

3.3 | SETD2 impairs EMT of LUAD cells

EMT is a conserved cellular process in which epithelial tumor cells lack polarity and transform into a mesenchymal phenotype. To demonstrate whether the SETD2 affected EMT, we used western blotting to assay the molecular marker levels of EMT (E-cadherin, N-cadherin, and vimentin). As shown in Figure 3A,B, the results displayed that SETD2 overexpression elevated E-cadherin level and decreased levels of N-cadherin and vimentin in A549 and H1975 cells (Figure 3A) while SETD2 knockdown inhibited levels of E-cadherin and enhanced levels of N-cadherin and vimentin in A549 and H1975 cells (Figure 3B), indicating that SETD2 could inhibit EMT. Moreover, this was further characterized by a morphological change from a spindle-shaped mesenchymal phenotype to a more epithelial-like, cobblestone phenotype, and an vimentin/E-cadherin switch (Figure 3C) in the SETD2 overexpressed A549 and H1975 cells using a confocal microscope.
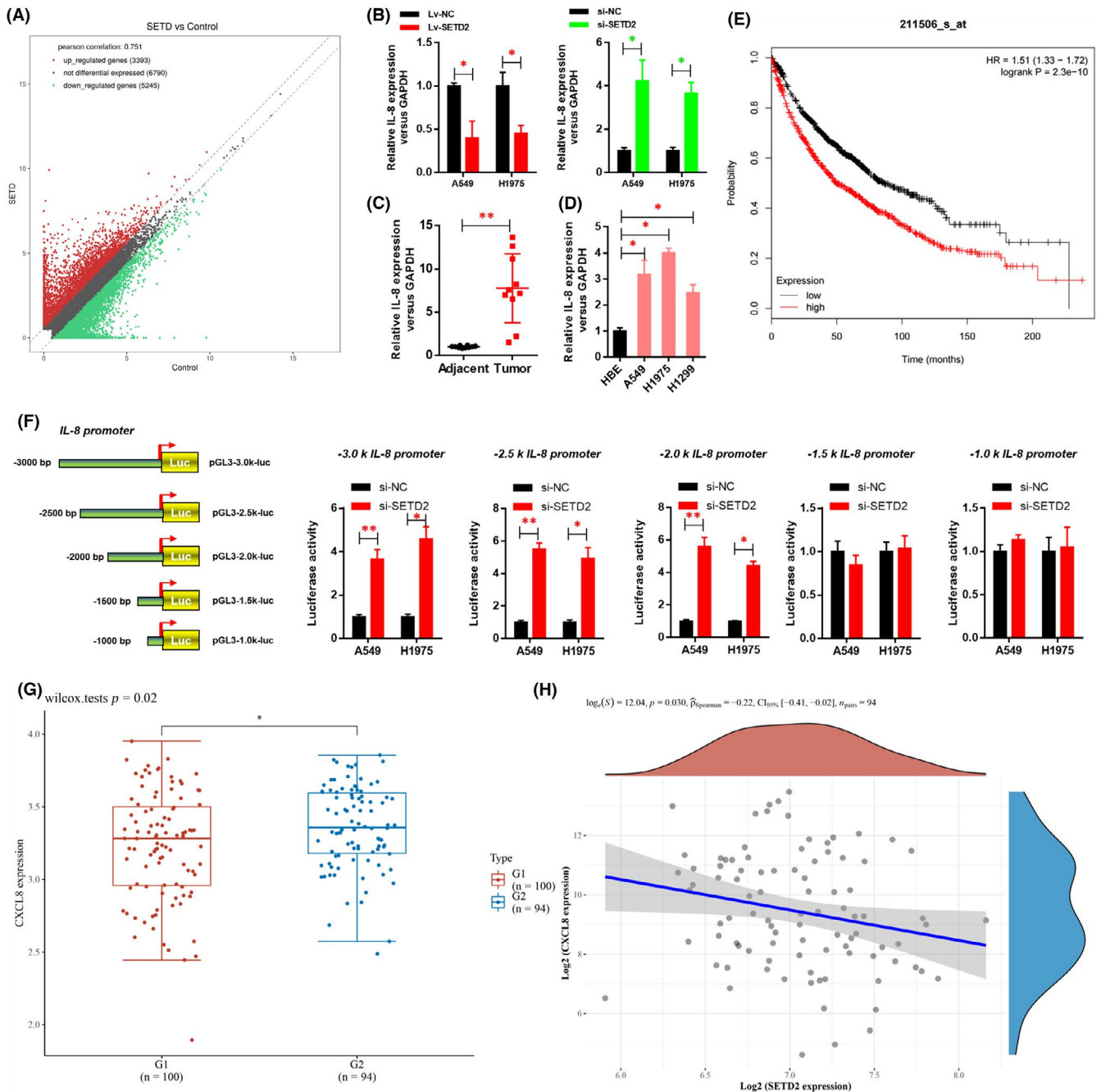
FIGURE 4 SETD2 transcriptionally inhibits the expression of IL-8. (A) IL-8 was downregulated upon SETD2 overexpression as indicated in the volcano plot. (B) The significantly upregulated IL-8 upon SETD2 knockdown and downregulated IL-8 in SETD2 overexpression were verified using real-time PCR. (C) The mRNA expression differences of IL-8 between lung tumors and adjacent normal tissues were analyzed using real-time PCR. (D) The mRNA expression differences in IL-8 between human lung cancer cell lines (A549, H1975 and H1299) and human bronchial epithelial cell line HBE were analyzed using real-time PCR. (E) Kaplan–Meier analyses were conducted to explore the correlation of IL-8 expression with overall survival of patients with NSCLC. (F) A schematic diagram showing the *IL-8* promoter luciferase reporter vectors with four distinct promoter regions, which then were co-transfected with siSETD2 or siNC into A549 and H1975 cells and subjected to luciferase activity assays. (G) The expression profile of lung cancer in the GEO database (ID: GSE40791) was used to evaluate the relationship between SETD2 and IL-8. (H) The correlation between the levels of IL-8 and SETD2 in lung tumors was analyzed. Data are presented as means ± SEM, $n = 3$; statistical significance: *$p < 0.05$, **$p < 0.01$

3.4 | SETD2 negatively regulates IL-8 expression

To get an insight into the molecular basis of SETD2 impairing lung cancer progression, we performed gene expression analysis using the

SETD2 overexpression and control A549 cells. As shown in the volcano plots (Figure 4A), IL-8 was found to be significantly downregulated upon SETD2 overexpression and upregulated by SETD2 knockdown (Figure 4B). We further found that IL-8 expression was significantly
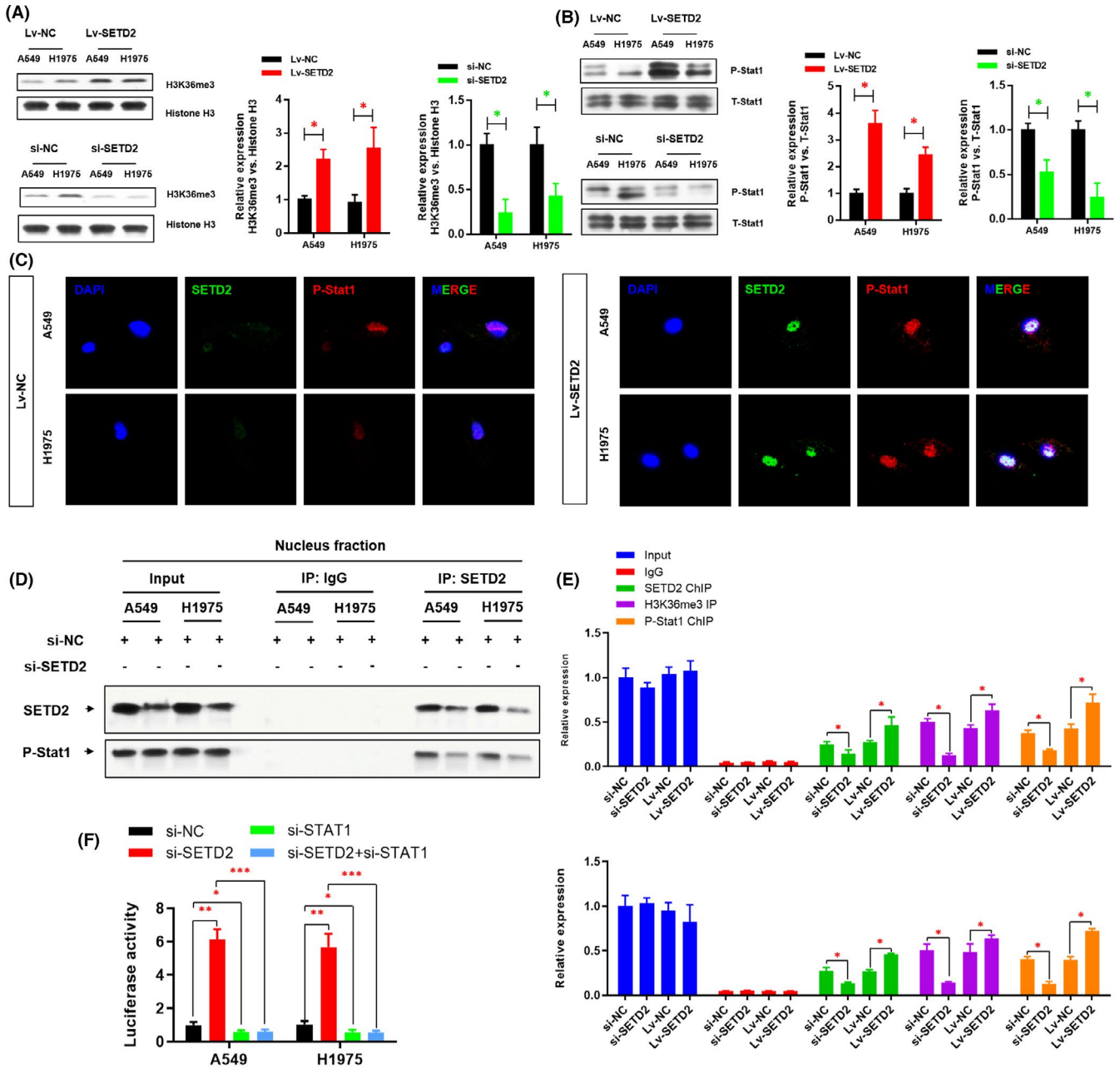
FIGURE 5 SETD2-mediated H3K36me3 prevents STAT1 from activating IL-8 expression. (A) The levels of H3K36me3 in the SETD2-overexpressed and -knockdown A549 and H1975 cells were evaluated using western blotting. (B) The phosphorylated levels of STAT1 in the SETD2-overexpressed and -knockdown A549 and H1975 cells were evaluated using western blotting. (C) The translocation of STAT1 into the nucleus in the SETD2-overexpressed A549 and H1975 cells was analyzed under a Zeiss confocal microscope. (D) The protein interaction between SETD2 and STAT1 in the SETD2-knockdown A549 and H1975 cells was evaluated using co-immunoprecipitation. (E) ChIP-qPCR assays of SETD2, H3K36me3, and STAT1 in the *IL-8* promoter in normal and SETD2-knockdown A549 and H1875 cells. (F) Luciferase report assays for the *IL-8* promoter in normal and SETD2-knockdown A549 and H1875 cells with or without STAT1 knockdown were performed. Data are presented as means ± SEM, $n = 3$; statistical significance: *$p < 0.05$, **$p < 0.01$

more highly expressed in tumor tissues (Figure 4C) and cell lines (Figure 4D), compared with that in normal tissues and HBE cells. Therefore, we hypothesized that IL-8 might be negatively regulated by SETD2. Kaplan–Meier analyses were further conducted to explore the correlation of IL-8 expression with overall survival of NSCLC patients. Kaplan–Meier survival analysis showed that the high IL-8 expression was associated with poor prognosis in patients with NSCLC

($p < 0.05$, Figure 4E). As mentioned previously, SETD2 catalyzed H3K36me3 to regulate gene transcription and was implicated in RNA splicing during gene transcription. Therefore, we sought to determine how SETD2 regulated IL-8 expression. Promoter activity assay showed that five truncations with different length of *IL-8* promoter (−1.0 k, −1.5 k, −2.0 k, −2.5 k and −3.0 k) were amplified and cloned into pGL3-basic vectors for luciferase reporter assays (Figure 4F). Results
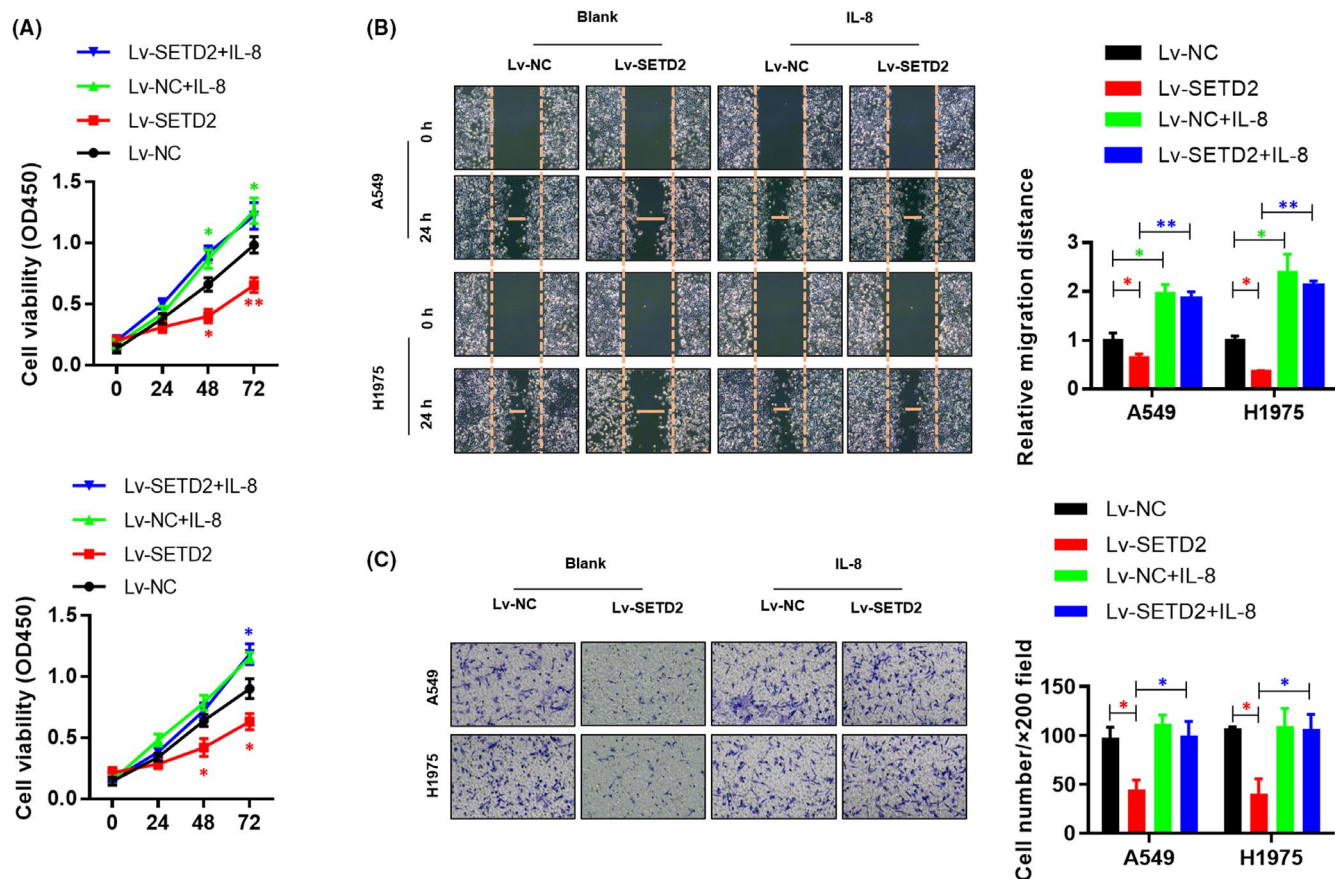
FIGURE 6 IL-8 administration reverses the impairment of SETD2 on the proliferation, migration, and invasion ability of LUAD cells. (A) The effects of IL-8 treatment with or without STED2 overexpression on the cell proliferation ability of A549 and H1975 cells were analyzed using a CCK-8 assay. (B) The effects of IL-8 treatment with or without STED2 overexpression on the cell migration ability of A549 and H1975 cells were analyzed using a wound healing assay. (C) The effects of IL-8 treatment with or without STED2 overexpression on the cell invasion ability of A549 and H1975 cells were analyzed using a transwell invasion assay. Data are presented as means $\pm$ SEM, $n = 3$; statistical significance: $*p < 0.05$, $**p < 0.01$

demonstrated that SETD2 ablation significantly increased the expression levels of −2.0 k, −2.5 k and −3.0 k *IL-8* promoter regions, while no changes were observed in the expression levels of −1.0 k and −1.5 k *IL-8* promoter regions (Figure 4F), suggesting that SETD2 negatively regulated *IL-8* expression via its −2.0 k to ~−1.0 k promoter region. To evaluate the relationship between SETD2 and IL-8, the expression profile of lung cancer in the Gene Expression Omnibus (GEO) database (ID: GSE40791) was used. The level of IL-8 in lung tumors was significantly higher than that in the normal lung tissues (Figure 4G) and negatively correlated with the level of SETD2 (Figure 4H). Taken together, these results revealed that SETD2-catalyzed H3K36me3 transcriptionally inhibited IL-8 transcription.

3.5 | SETD2-mediated H3K36me3 prevents STAT1 from activating IL-8 expression

To understand how H3K36me3 negatively regulated IL-8 expression, we first confirmed that SETD2-catalyzed H3K36me3 was associated with IL-8 expression. Western blotting analyses were performed using cell lysates from A549 and H1975 cells with or

without SETD2 overexpression or knockdown. Results indicated that the H3K36me3 levels were significantly increased or reduced upon SETD2 overexpression and knockdown, respectively (Figure 5A), as the *IL-8* promoters contained binding sequences for STAT1. Moreover, activation of the JAK–STAT1 signaling pathways stimulated IL-8 transcription. Therefore, we next investigated the role of STAT1 in SETD2-inhibited IL-8 expression. Western blot analysis revealed that the phosphorylation levels of STAT1 were significantly increased or reduced upon SETD2 overexpression and knockdown, respectively (Figure 5B). It is well established that STAT family members are phosphorylated by receptor associated kinases, and then form homodimers or heterodimers that translocate to the cell nucleus where they act as transcription activators. Therefore, translocation of STAT1 into the nucleus was analyzed using a Zeiss confocal microscope. As expected, SETD2 overexpression obviously increased the phosphorylation levels of STAT1 in the nucleus in the A549 and H1975 cells (Figure 5C). Moreover, co-immunoprecipitation (co-IP) experiments in A549 and H1975 cells using antibodies against SETD2 showed that SETD2 co-located with STAT1, and that this was dramatically diminished by SETD2 downregulation (Figure 5D). In addition, independent ChIP-qPCR results showed enrichment of the *IL-8* promoter in anti-SETD2,
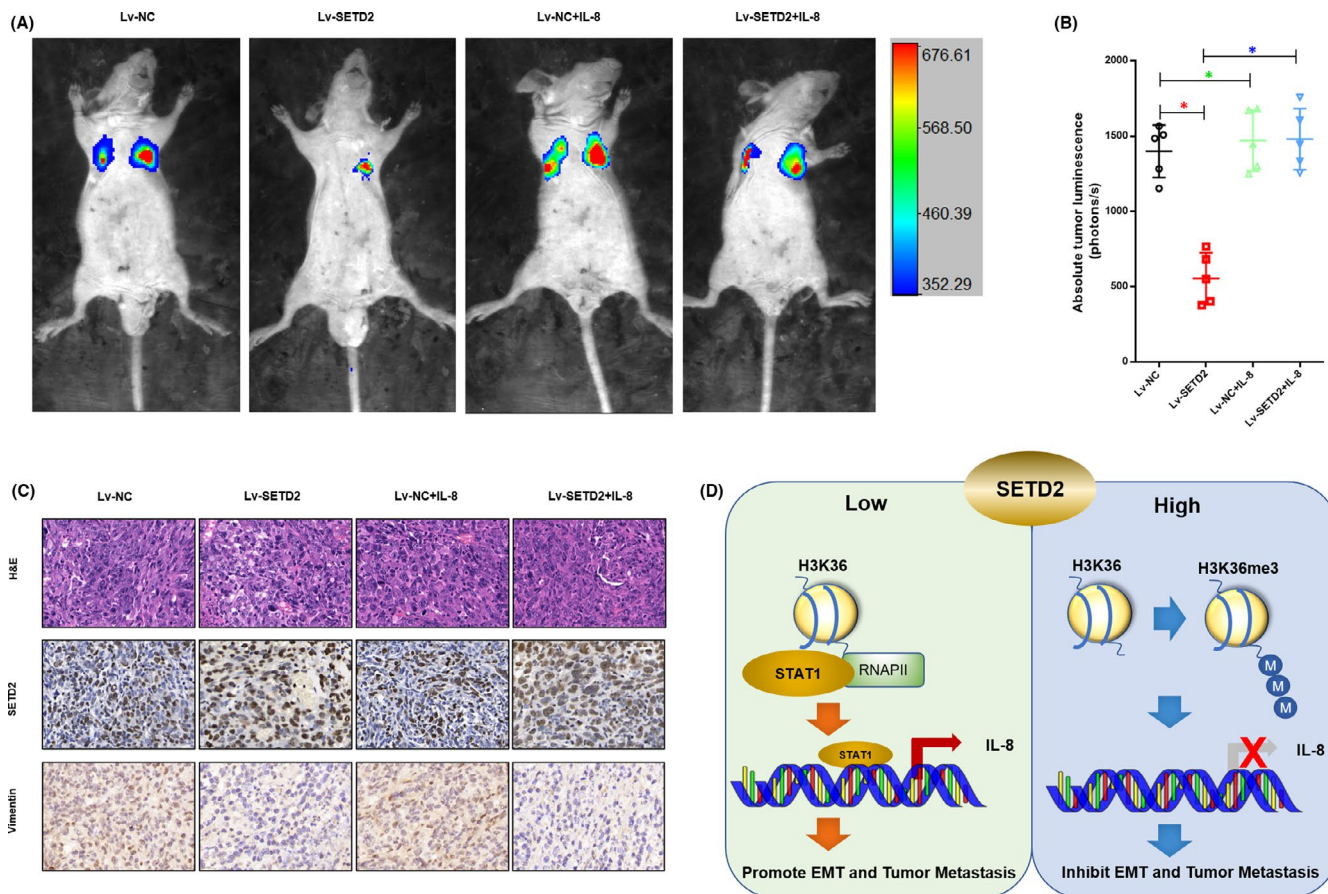
FIGURE 7 *In vivo* verification of the tumorigenesis inhibition of SETD2-IL8 axis in LUAD. (A) Representative image of bioluminescent imaging mice injected with SETD2-overexpressing (Lv-SETD2), IL-8-overexpressing (Lv-IL-8), or SETD2/IL-8 double overexpressing (Lv-SETD2+IL-8) A549 cells. (B) The bioluminescence intensities in these four mice groups were counted. (C) H&E, SETD2, and vimentin staining of subcutaneous tumors of control and SETD2-overexpressing A548 cells with or without IL-8 treatment. Scale bars, 50 μm. (D) Graphic model of SETD2 functions in LUAD. SETD2-mediated H3K36me3 prevents the assembly of Stat1 on the *IL-8* promoter and contributes to the inhibition of tumorigenesis in lung adenocarcinoma. Data are presented as means ± SEM, $n = 3$; statistical significance: $^*p < 0.05$; $^{**}p < 0.01$

H3K36me3, and STAT1 ChIP assays (Figure 5E), which were similarly decreased in the SETD2-knockdown A549 and H1975 cells (Figure 5E). Consistently, SETD2-knockdown elevated *IL-8* promoter activity in A549 cells was obviously abolished by STAT1 knockdown (Figure 5F). Taken together, these results revealed that SETD2-mediated H3K36me3 prevented STAT1 from activating IL-8 expression.

treatment in A549 and H1975 cells. However, STAT1 overexpression failed to alter the SETD2-impaired cell viability, migration, invasion, and EMT in A549 and H1975 cells (Figure S1A–D). By contrast, STAT1 knockdown or IL-8 neutralized antibody (IL-8 Abs) significantly reversed SETD2-overexpression improved cell viability, migration, invasion, and EMT in A549 and H1975 cells (Figure S2A–D).

3.6 | IL-8 administration reverses the impairment of SETD2 on proliferation, migration, and invasion ability of LUAD cells

To evaluated the critical role of IL-8 in the SETD2 impaired proliferation, migration, and invasion ability of LUAD cells, we next detected the effect of exogenous IL-8 treatment in SETD2-overexpressed LUAD cells, compared with vector control LUAD cells. As shown in Figure 6A, the SETD2-impaired cell viability of LUADs was obviously rescued using endogenous IL-8 treatment. Similarly, the decreased migration (Figure 6B) and invasion (Figure 6C) caused by SETD2 overexpression eventually rose again with endogenous IL-8

3.7 | *In vivo* verification of the tumorigenesis inhibition of SETD2-IL8 axis in LUAD

We further validated the regulatory relationship between SETD2 and IL-8 in a nude mice xenograft model. SETD2 and IL-8 were ectopically overexpressed separately or simultaneously in luciferase-labeled A549 cells to establish the SETD2-overexpressing (Lv-SETD2), IL-8-overexpressing (Lv-IL-8) and SETD2/IL-8 double overexpressing (Lv-SETD2+IL-8) A549 cells, which were subcutaneously injected into nude mice by tail vein injection. SETD2 overexpression resulted in a significant reduction in tumor metastasis, whereas intermittent therapy with IL-8 alone had no significant

effect on tumor metastasis reduction, but reversed the SETD2-inhibited tumor metastasis, as measured using bioluminescent imaging (Figure 7A). Bioluminescence counts were strongly correlated with tumor metastasis (Figure 7B). H&E staining and IHC staining confirmed the expression levels of SETD2 and vimentin in these tumors (Figure 7C). These results collectively suggested the modulatory effects of the SETD2/STAT1/IL-8 axis on tumor growth and metastasis in LUAD (Figure 7D).

4 | DISCUSSION

LUAD's tumorigenesis is thought to require multiple subsequent mutations in genes associated with cell growth, differentiation, and survival.[22,23] Some studies have shown that H3K36 methylation is associated with abnormal differentiation or proliferation.[10] It has been reported that the absence of SETD2 would impair the differentiation of ES cells, while the expression of H3.3 mutants that inhibited the methylation of H3K36 would impair the differentiation of chondrocytes and mesenchymal progenitors.[24] SETD2 and its catalyzed H3K36me3 play crucial roles in maintaining chromosome integrity and regulating gene transcription.[25,26] Mutations and deletions of the *SETD2* gene have been identified in several cancers.[27-31] In a very recent study, SETD2 was reported to inhibit colon cancer by modulating alternative splicing.[20] Moreover, SETD2 was reported to directly mediate STAT1 methylation on lysine 525 via its methyltransferase activity, which reinforced IFN-activated STAT1 phosphorylation and antiviral cellular responses.[12] However, the roles of SETD2 loss in the progression of LUAD have not been well established. Here, we determined that SETD2 was significantly decreased in LUAD. SETD2 loss greatly upregulated IL-8 expression via its enzymatic activity in catalyzing H3K36me3, which bound STAT1 to the *IL-8* promoter and activated its expression (Figure 7D).

IL-8 is a pro-inflammatory CXC chemokine associated with the promotion of neutrophil chemotaxis and degranulation.[32] This chemokine activates multiple intracellular signaling pathways downstream of G-protein-coupled receptors on both cell surfaces.[33] Increased expression of IL-8 and/or its receptors in cancer cells, endothelial cells, infiltrating neutrophils, and tumor-associated macrophages suggests that IL-8 may play an important regulatory role in the tumor microenvironment.[34] Therefore, IL-8 signaling increases the proliferation and survival of cancer cells and enhances the migration and metastasis of cancer cells, endothelial cells, and invasive neutrophils at tumor sites. In addition, stress and drug-induced IL-8 signaling pathways have been shown to confer chemotherapy resistance in cancer cells.[35] Therefore, unveiling the upstream regulation of IL-8 signaling may be a significant therapeutic intervention in the prevention of tumor progression. Moreover, mice do not have the *IL-8* gene, so human cancer cell lines and xenograft studies have been used to study the role of IL-8 in carcinogenesis.[36,37] In this study, we identified that SETD2-mediated H3K36me3 could prevent transcription factor STAT1 assembly on the *IL-8* promoter, which impaired the activation of IL-8. Furthermore, IL-8 treatment obviously reversed the inhibitory effect of SETD2 in the proliferation and metastasis of LUAD cells *in vitro* and in xenografts.

Tumor EMT is a phenotypic transformation that promotes the acquisition of fibroblast-like morphology by epithelial tumor cells, thereby enhancing the motility and aggressivity of tumor cells, enhancing metastasis tendency and resistance to chemotherapy, radiotherapy, and some small-molecule targeted therapies.[38,39] Evidence suggests that an autocrine-positive ring exists between IL-8 and the EMT transcription factor Brachyury in breast and lung cancer cell lines, which has been well documented. The addition of purified IL-8 to cancer cells has been shown to increase the percentage of aldehyde-positive cells and enhance the migration and invasiveness of cancer cells *in vitro*.[40-42] In this study, we demonstrated that IL-8 is negatively regulated by SETD2-mediated H3K36me3. Using *in vivo* xenograft experiments, we also confirmed that IL-8 administration significantly reversed the inhibitory of EMT by SETD2. In summary, our findings highlighted the suppressive role of SETD2/H3K36me3 in cell proliferation, migration, invasion, and EMT during LUAD carcinogenesis, via regulation of the STAT1–IL-8 signaling pathway. Therefore, our studies on the molecular mechanism of SETD2 will advance our understanding of epigenetic dysregulation at LUAD development.

CONFLICT OF INTEREST

The authors declare no conflict of interest.

AUTHOR CONTRIBUTIONS

R. Chen, Y. Chen, M. Ji and X. Yang designed this study. R. Chen and Y. Chen performed all experiments. X. Yang collected tissue samples and the clinical data. R. Chen, Y. Chen, C. Wu, Q. Li, J. Wu, W-w. Hu, W-q. Zhao and W. Wei analyzed and interpreted the data; R. Chen and X. Yang drafted the manuscript. All authors read and approved the final manuscript.

ETHICAL APPROVAL

LUAD tissues and paired adjacent normal epithelial tissues were acquired from the Third Affiliated Hospital of Soochow University from 2003 to 2015. Tissue specimens were obtained through puncture and stored in liquid nitrogen at −80°C. All experiments using the human tissues were conducted under the approval of the Third Affiliated Hospital of Soochow University. All patients gave informed consent. The animal experiments were approved by the Institutional Animal Care and Use Committee of the Third Affiliated Hospital of Soochow University.

CONSENT FOR PUBLICATION

Written consents for publication were obtained from all the patients involved in our study.

DATA AVAILABILITY STATEMENT

All data in our study are available upon request.

ORCID

Xin Yang https://orcid.org/0000-0002-3440-085X
Yan Chen https://orcid.org/0000-0003-1950-3903

REFERENCES

1. Siegel RL, Miller KD, Jemal A. Cancer statistics, 2019. *CA Cancer J Clin*. 2019;69:7-34.
2. Siegel RL, Miller KD, Jemal A. Cancer statistics, 2020. *CA Cancer J Clin*. 2020;70:7-30.
3. Chen W, Zheng R, Baade PD, et al. Cancer statistics in China, 2015. *CA Cancer J Clin*. 2016;66:115-132.
4. MRD may predict relapse in NSCLC. *Cancer Discov*. 2020;10:OF7.
5. Revannasiddaiah S, Devadas SK, Maka VV. Osimertinib in EGFR-mutated advanced NSCLC. *N Engl J Med*. 1864;2020:382.
6. Rosell R, Chaib I, Santarpia M. Targeting MET amplification in EGFR-mutant non-small-cell lung cancer. *Lancet Respir Med*. 2020;8(11):1068-1070.
7. Neri F, Rapelli S, Krepelova A, et al. Intragenic DNA methylation prevents spurious transcription initiation. *Nature*. 2017;543(7643):72-77.
8. Frye M, Harada BT, Behm M, He C. RNA modifications modulate gene expression during development. *Science*. 2018;361:1346-1349.
9. Ling C, Ronn T. Epigenetics in human obesity and type 2 diabetes. *Cell Metab*. 2019;29:1028-1044.
10. Wagner EJ, Carpenter PB. Understanding the language of Lys36 methylation at histone H3. *Nat Rev Mol Cell Biol*. 2012;13:115-126.
11. Baylin SB, Jones PA. A decade of exploring the cancer epigenome — biological and translational implications. *Nat Rev Cancer*. 2011;11:726-734.
12. Chen K, Liu J, Liu S, et al. Methyltransferase SETD2-mediated methylation of STAT1 Is critical for interferon antiviral activity. *Cell*. 2017;170(3):492-506.e14.
13. Huang KK, McPherson JR, Tay ST, et al. SETD2 histone modifier loss in aggressive GI stromal tumours. *Gut*. 2016;65:1960-1972.
14. Park IY, Powell RT, Tripathi DN, et al. Dual chromatin and cytoskeletal remodeling by SETD2. *Cell*. 2016;166:950-962.
15. Pfister SX, Ahrabi S, Zalmas LP, et al. SETD2-dependent histone H3K36 trimethylation is required for homologous recombination repair and genome stability. *Cell Rep*. 2014;7:2006-2018.
16. Chen R, Zhao WQ, Fang C, Yang X, Ji M. Histone methyltransferase SETD2: a potential tumor suppressor in solid cancers. *J Cancer*. 2020;11:3349-3356.
17. Joshi AA, Struhl K. Eaf3 chromodomain interaction with methylated H3–K36 links histone deacetylation to Pol II elongation. *Mol Cell*. 2005;20:971-978.
18. Keogh MC, Kurdistani SK, Morris SA, et al. Cotranscriptional set2 methylation of histone H3 lysine 36 recruits a repressive Rpd3 complex. *Cell*. 2005;123:593-605.
19. Xu Q, Xiang Y, Wang Q, et al. SETD2 regulates the maternal epigenome, genomic imprinting and embryonic development. *Nat Genet*. 2019;51:844-856.
20. Yuan H, Li N, Fu D, et al. Histone methyltransferase SETD2 modulates alternative splicing to inhibit intestinal tumorigenesis. *J Clin Invest*. 2017;127:3375-3391.
21. Zhu K, Lei PJ, Ju LG, et al. SPOP-containing complex regulates SETD2 stability and H3K36me3-coupled alternative splicing. *Nucleic Acids Res*. 2017;45:92-105.
22. Coudray N, Ocampo PS, Sakellaropoulos T, et al. Classification and mutation prediction from non-small cell lung cancer histopathology images using deep learning. *Nat Med*. 2018;24:1559-1567.
23. Hu K, Li K, Lv J, et al. Suppression of the SLC7A11/glutathione axis causes synthetic lethality in KRAS-mutant lung adenocarcinoma. *J Clin Invest*. 2020;130:1752-1766.
24. Zhang Y, Xie S, Zhou Y, et al. H3K36 histone methyltransferase Setd2 is required for murine embryonic stem cell differentiation toward endoderm. *Cell Rep*. 2014;8:1989-2002.
25. Fang D, Gan H, Lee JH, et al. The histone H3.3K36M mutation reprograms the epigenome of chondroblastomas. *Science*. 2016;352:1344-1348.
26. Lu C, Jain SU, Hoelper D, et al. Histone H3K36 mutations promote sarcomagenesis through altered histone methylation landscape. *Science*. 2016;352:844-849.
27. Licht JD. SETD2: a complex role in blood malignancy. *Blood*. 2017;130:2576-2578.
28. Morris MR, Latif F. The epigenetic landscape of renal cancer. *Nat Rev Nephrol*. 2017;13:47-60.
29. Niu N, Lu P, Yang Y, et al. Loss of Setd2 promotes Kras-induced acinar-to-ductal metaplasia and epithelia-mesenchymal transition during pancreatic carcinogenesis. *Gut*. 2020;69:715-726.
30. Patnaik MM, Abdel-Wahab O. SETD2 - linking stem cell survival and transformation. *Cell Res*. 2018;28:393-394.
31. Zhang YL, Sun JW, Xie YY, et al. Setd2 deficiency impairs hematopoietic stem cell self-renewal and causes malignant transformation. *Cell Res*. 2018;28:476-490.
32. Bakouny Z, Choueiri TK. IL-8 and cancer prognosis on immunotherapy. *Nat Med*. 2020;26:650-651.
33. Abraham RT. Chemokine to the rescue: interleukin-8 mediates resistance to PI3K-pathway-targeted therapy in breast cancer. *Cancer Cell*. 2012;22:703-705.
34. Dolgin E. BMS bets on targeting IL-8 to enhance cancer immunotherapies. *Nat Biotechnol*. 2016;34:1006-1007.
35. Yuen KC, Liu LF, Gupta V, et al. High systemic and tumor-associated IL-8 correlates with reduced clinical benefit of PD-L1 blockade. *Nat Med*. 2020;26:693-698.
36. Asfaha S, Dubeykovskiy AN, Tomita H, et al. Mice that express human interleukin-8 have increased mobilization of immature myeloid cells, which exacerbates inflammation and accelerates colon carcinogenesis. *Gastroenterology*. 2013;144:155-166.
37. Modi WS, Yoshimura T. Isolation of novel GRO genes and a phylogenetic analysis of the CXC chemokine subfamily in mammals. *Mol Biol Evol*. 1999;16:180-193.
38. Brabletz T, Kalluri R, Nieto MA, Weinberg RA. EMT in cancer. *Nat Rev Cancer*. 2018;18:128-134.
39. Dongre A, Weinberg RA. New insights into the mechanisms of epithelial-mesenchymal transition and implications for cancer. *Nat Rev Mol Cell Biol*. 2019;20:69-84.
40. McFaline-Figueroa JL, Hill AJ, Qiu X, Jackson D, Shendure J, Trapnell C. A pooled single-cell genetic screen identifies regulatory checkpoints in the continuum of the epithelial-to-mesenchymal transition. *Nat Genet*. 2019;51:1389-1398.
41. Su J, Morgani SM, David CJ, et al. TGF-beta orchestrates fibrogenic and developmental EMTs via the RAS effector RREB1. *Nature*. 2020;577:566-571.
42. Yang J, Antin P, Berx G, et al. Guidelines and definitions for research on epithelial-mesenchymal transition. *Nat Rev Mol Cell Biol*. 2020;21:341-352.